F2014-CET-161

SENSITIVITY ANALYSIS OF A QUASI-DIMENSIONAL MODEL FOR SI ENGINES FUELLED WITH GASOLINE-ALCOHOL BLENDS

[1]Sileghem, Louis[*]; [1]Vancoillie, Jeroen; [1]Verhelst, Sebastian;
[1] Department of Flow, Heat and Combustion Mechanics, Ghent University, Belgium

KEYWORDS – Alcohol fuel, Spark Ignition Engine, Thermodynamic, Modelling

ABSTRACT – Methanol and ethanol are interesting spark-ignition engine fuels, both from a production and an end-use point of view. Despite promising experimental results, the full potential of these fuels remain to be explored. In this respect, quasi-dimensional engine simulation codes are especially useful as they allow cheap and fast optimization of engines. Since methanol and ethanol have different properties compared to gasoline, it is important to know how to modify simulation models currently calibrated for gasoline operation to operate on gasoline-alcohol blends or pure alcohols. The aim of the current work was to do a sensitivity analysis of a quasi-dimensional model for spark ignition engines running on gasoline-alcohol blends. Therefore a new correlation for the laminar burning velocity of gasoline-alcohol blends is implemented in the quasi-dimensional model. Several factors (such as the laminar burning velocity, initial flame kernel, residual gas fraction, turbulence…) have been investigated and the sensitivity of these factors and the used submodels on the predictive performance was assessed for different gasoline-methanol blends. The results show the importance of the laminar burning velocity correlation, the initial flame kernel and the estimation of the residual gas fraction.

TECHNICAL PAPER –

INTRODUCTION

The use of sustainable liquid alcohols in spark-ignition engines offers the potential of decarbonizing transport and securing domestic energy supply while increasing engine performance and efficiency compared to fossil fuels thanks to a number of interesting properties [1]. The most significant interesting properties of light alcohols include:

- High heat of vaporization, which causes considerable charge cooling as the injected fuel evaporates
- Elevated knock resistance, which allows to apply higher compression ratios, optimal spark timing and aggressive downsizing.
- High flame speeds, enabling qualitative load control using mixture richness or varying amounts of exhaust gas recirculation (EGR).

Driven by the Renewable Energy Directive in the EU [2] and The Energy Independence and Security Act in the US [3], biofuels like ethanol are likely to be used at increasingly high concentrations in gasoline over the next years due to the compatibility with modern vehicles and the distribution and fueling infrastructure. For now, bio-ethanol has the lion's share when it comes to non-petroleum-derived transportation energy. Despite of the projected growth, bio-ethanol is not considered to be viable in the long term as a substitute for fossil fuels, due to the biomass limit [4]. This biomass limit is different for each country, and depends on the amount of biomass that can be grown there, the amount of energy required by the country, any impact of land-use change that may arise, and limits set by any impact on the food chain [5], [6]. It has been estimated that this limits the potential of biofuels to about 20% of the energy demand in 2050 [7].

Compared to ethanol, methanol is actually more versatile from a production point of view. Methanol can be produced from a wide variety of renewable sources (e.g. gasification of wood, agricultural by-products and municipal waste) and alternative fossil fuel based feed stocks (e.g. coal and natural gas). A number of workers have even proposed a sustainable closed-carbon cycle where methanol is synthesized from hydrogen, produced from renewable electricity, and atmospheric CO_2, thus forming a liquid hydrogen carrier and making it an 'electrofuel' [8].
Methanol has been successfully used in large-scale fleet trials [9] and the potential of neat light alcohol fuels (methanol and ethanol) and alcohol-gasoline blends has been demonstrated experimentally in both dedicated and flex-fuel alcohol engines [10, 11].
Despite promising experimental results, the full potential of alcohol fuels and their impact on engine control strategies remain to be explored, especially since advanced engines incorporate a host of technologies and thus many degrees of freedom for engine optimization. Today these issues can be addressed at low cost using system simulations of the whole engine, provided that the employed models account for the effect of the fuel on the combustion process.

In this respect quasi-dimensional engine simulation codes are especially useful as they are well suited to evaluate existing engines, performing parameter studies and predicting optimum engine settings without resorting to complex multidimensional models [12]. At Ghent University, a quasi-dimensional code (Ghent University Engine Simulation Tool or GUEST code) for the power cycle of engines fuelled with hydrogen or pure (m)ethanol has been developed and validated during earlier work [13-15]. The current work aims to extend this code to (m)ethanol-gasoline blends. In this paper elements of this work pertaining to the power cycle simulation of engines running on methanol-gasoline blends are presented.

SIMULATION PROGRAM

Framework and assumptions - The focus in this paper is an analysis of the power cycle model for engine operation on methanol-gasoline blends.
The in-house GUEST code was coupled to a commercial gas dynamics simulation tool (GT-Power [16]) during the current work, to enable simulation of the entire engine cycle.

The current two-zone quasi-dimensional power cycle model was derived using several standard assumptions, as mentioned in [12, 13]. The equations for the rate of change of the cylinder pressure $dp/d\theta$, burned and unburned temperatures, $dT_b/d\theta$ and $dT_u/d\theta$, are derived from conservation of energy. Additionally, a number of models and assumptions are necessary to close these equations:

- Heat exchange is calculated separately for the cylinder liner, cylinder head and piston based on an extension of the Woschni model discussed in [17]
- The CFR (Cooperative Fuel Research) engine used for validation of the simulation (see later) has a simple disc-shaped combustion chamber and ran at a fixed speed of 600 rpm. Therefore turbulence quantities are calculated using a very simple turbulence model based on measurements done in a similar engine [18]. The integral length scale Λ is kept constant at 1/5 of the minimum clearance height, and the rms turbulent velocity u' linearly decreases according to:
  $$u' = u'_{TDC}[1 - 0.5(\theta - 360)/45] \quad (1)$$
  Where u'_{TDC} is the rms turbulent velocity at top dead centre (TDC), taken to be 0.75 times the mean piston speed, θ is the crank angle (360 at TDC of compression).

- The mass burning rate is derived from a turbulent combustion model. The one used in this work is based on the entrainment framework, where the rate of entrainment of unburned gas into the flame front is given by

$$\frac{dm_e}{d\theta} = \rho_u A_f u_{te} \quad (2)$$

Where m_e is the entrained mass, A_f is the mean flame front surface, and u_{te} is the turbulent entrainment velocity (see later). The mass entrained into the flame front is then supposed to burn with a rate proportional to the mass of entrained unburned gas, with a time constant τ_b:

$$\frac{dm_b}{d\theta} = (m_e - m_b)/\tau_b \quad (3)$$

$$\tau_b = \lambda_T / u_l \quad (4)$$

u_l is the laminar burning velocity and λ_t is the Taylor length scale, given by:

$$\lambda_t = C_3 \Lambda / \sqrt{Re_t} \quad (5)$$

$$Re_t = u' \Lambda / \nu_u \quad (6)$$

Where C_3 is a calibration constant, Λ is the integral turbulent length scale and ν_u is the kinematic viscosity of the unburned gases. Equations (2) and (3) are used as a mathematical representation of the effects of a finite flame thickness [13].

- Gas properties are taken from the standard GT-Power libraries [16]
- For simplicity, blowby rates and the influence of crevice volumes have been neglected.

If one is primarily interested in the indicated work and efficiency, in other words simulation of the complete engine cycle, the ignition of the cylinder charge is usually not modeled in detail. In fact generally, the ignition is not modeled at all; but rather the start of combustion is initialized by assuming the instantaneous formation of an ignition kernel at or shortly after the ignition timing. The ignition kernel is often ascribed a certain mass or volume [12].
In this study, $2r_f$ = 1 mm was used as a starting point of the ignition kernel size. In a later stage, this initial flame kernel will be optimized.
Turbulent burning velocity model - A turbulent entrainment velocity u_{te} is needed for closure of Equation (2).
In the study, the combustion model of Wahiduzzaman et al. [19] is used. This is the standard combustion model in the simulation program GT-power. The commercial software GT-power will also be used to calculate the internal exhaust gas recirculation. The turbulent entrainment velocity is formed from the sum of the turbulent and the laminar burning velocities. The entrained mass rate of unburned gas becomes:

$$\frac{dm_e}{d\theta} = \rho_u A_f (u_t + u_n) \quad (7)$$

u_t is the turbulent burning velocity, assumed to be proportional to the rms turbulent velocity and u_n is the stretched laminar burning velocity:

$$\frac{dm_e}{d\theta} = \rho_u A_f (C_2 u' + u_n) \quad (8)$$

In the previous equation, C_2 is a calibration constant.
A flame propagating after spark ignition is first only wrinkled by the smallest scales of turbulence. For the simulations done in this work, a flame development multiplying factor for the turbulent burning velocity was used. u_t becomes:

$$u_t = C_2 u' \left(1 - \frac{1}{1 + C_k R_f^2 / \Lambda^2}\right) \quad (9)$$

Where R_f is the flame radius and C_k is calculated from the following expression:

$$C_k = \frac{C_1}{1+6H}\left(1 - e^{-4.81r^2}\right).(1.228 + 0.385r) \quad (10)$$

In the previous equation r is the ratio of turbulence length scale to flame thickness and H is a stretch factor. More information can be found in Wahiduzzaman et al. [19].

Several models exist for the turbulent entrainment velocity [13] and for the turbulent flame development. Although this could have an influence on the outcome of the study, the comparison of different turbulent entrainment velocity models and turbulent flame development models falls outside the scope of this study.

Laminar burning velocity correlation –One of the key parameters to model the combustion of fuels in spark ignition engines is the laminar burning velocity of the fuel. This is a physico-chemical property of a fuel-air-residuals mixture and thus a fundamental building block of any predictive engine model. A convenient way to implement laminar burning velocity data in a quasi-dimensional engine cycle code is by using a correlation which gives the laminar burning velocity in terms of pressure, temperature and composition of the unburned mixture. There are a lot of publications where a quasi-dimensional engine cycle model is used but few can be adapted easily to add an additional fuel component or do simulations over the whole blending range. Bougrine et al. [20] used also their quasi-dimensional model for blends of gasoline and ethanol with ethanol volume fractions ranging from 0% to 30%. They used the corrected correlation proposed by Gülder [21] for ethanol-isooctane blends. To do a parametric study of the blend ratio with higher alcohol fractions, a simple mixing rule for the laminar burning velocity of alcohol fuels would be interesting especially if other components such as methanol are added in the fuel as proposed by Turner et al. [5]. In the quasi-dimensional model of Ma et al. [22] and Perini et al [23], a simple mixing rule proposed by Benedetto et al. [24] was used for the laminar burning velocity of hydrogen-methane mixtures for a part of the mixing range.
If the effect of fuel blend composition or the effect of additional components has to be determined, simple mixing rules are needed that can predict the laminar burning velocity of the blends out of the correlations of the pure fuels with a good accuracy and without being computationally too demanding.
Sileghem et al. [25, 26] investigated if mixing rules could be used to determine the laminar burning velocity of fuel blends from the burning velocity of the fuel components. Sileghem et al. found that for (m)ethanol-hydrocarbon blends a mixing rule based on the energy fraction of each component was accurate enough. The laminar burning velocity of the alcohol-hydrocarbon blends can be determined as follows:

$$u_{l,blend}(\Phi) = \sum_{i=1}^{n} \alpha_i . u_{l,i}(\Phi) \quad (11)$$

In this expression α_i is the energy fraction of fuel component i. The energy fraction can be calculated as follows:

$$\alpha_i = \frac{\Delta cH_i^{\circ}.x_i}{\sum_{i=1}^{n} \Delta cH_i^{\circ}.x_i} \quad (12)$$

cHi° is the heat of combustion and x_i is the mole fraction of the fuel component i. In this study this mixing rule will be used in the quasi-dimensional simulations.
Two other mixing rules gave also results in good agreement with the experimental determinations of the laminar burning velocities for mixtures. More information can be found in [25-27].

In this study, we wanted to have a correlation for gasoline and a correlation for methanol from the same source to be able to compare the influence of temperature, pressure and diluent factors of the two correlations. Therefore two new correlations were built.
Both the laminar burning velocity of methanol and the gasoline used for the engine measurements have been determined using the heat flux method on a flat flame adiabatic burner [26, 27].
The form of the developed correlation is given by:

$$u_l = u_{l0}\left(\frac{T_u}{T_0}\right)^{\alpha}\left(\frac{p}{p_0}\right)^{\beta}(1-\gamma f) \quad (13)$$

Where u_{l0} and α are third order polynomials of ϕ fitted to the measurements done on the flat flame adiabatic burner. β is a first order function of ϕ taken from the recent study performed by Galmiche et al. [28] in which the pressure dependency of iso-octane was investigated and γ is a constant equal to 2.1 based on the measurements of Metghalchi and Keck [29] and found in many laminar burning velocity correlations.

Turbulent burning velocity models need (stretched) laminar burning velocity data of the air/fuel/residuals mixture at the instantaneous pressure and temperature. This implies the need for either a library of stretched flamelets or a model for the effect of stretch. Calculating the local flame speed from stretch-free data and a stretch model requires stretch-free data, naturally. As of today, there are insufficient data on stretch-free burning velocities at engine conditions, for any fuel. Stretch and instabilities hamper the experimental determination of stretch-free data at higher (engine-like) pressures [30]. This was one of the reasons to perform a sensitivity analysis. In this way, it can be investigated how precise experimental determination of stretch-free data has to be. No stretch model has been implemented in the code as of yet, partly because of a lack of reliable data regarding the effect of stretch on methanol-gasoline flames at engine-like conditions [31].

ENGINE TEST

Engine - To analyze the combustion model's predictive capabilities, a series of measurements were done on a port fuel injected single cylinder CFR engine, described in [32]. The main characteristics of this engine are summarized in Table 1.

Bore	82.55 mm
Stroke	114.2 mm
Swept Volume	611.7 cm³
Geometry	Disc-shaped
Speed	600 rpm
IVO/IVC	17 °CA ATDC / 26 °CA ABDC
EVO/EVC	32 °CA BBDC / 6°CA ATDC

Table 1: Characteristics of the single cylinder CFR engine

The measurements comprise variable fuel/air equivalence ratio ϕ and methanol-gasoline ratio. Measurements were done for M0, M20, M40, M60, M80 and M100 at lambda equal to 1, 1.2 and 0.8. Ignition timing was fixed at 12° BTDC and the throttle was turned open with 10°. In order to allow an accurate comparison, all measurements were performed on the same day and all parameters were fixed except for the injection duration and the fuel composition.

Model setup - As the main focus of the current work was to evaluate the combustion model, the employed engine model is limited to the closed part of the engine cycle (IVC to EVO). The initial conditions for mass fractions of air and fuel, the mean temperature and pressure are taken from the measurements. The residual gases (from the previous engine cycle) are calculated using a Three Pressure Analysis in the GT-power software. To perform a three pressure analysis in GT-POWER, three different pressure measurements are required from the

cylinder of interest. Two of these measurements are port pressures (intake and exhaust) and the third is cylinder pressure. The main purpose of this type of simulation is to analyze the measurements in order to obtain a single combustion burn rate for each operating condition. This burn rate can be used to compare it with the predictive burn rate that will come out of the predictive model. This analysis is also very good for an estimation of the internal EGR.

Calibration of the predictive model - The calibration sets the coefficients for the heat transfer model, the flame development model (C_1) and the turbulent burning velocity model (C_2, C_3). Since it is interesting to know how to modify simulation models currently calibrated for gasoline operation to operate on gasoline-alcohol blends or pure alcohols, it was decided to calibrate the code only for one operation point on gasoline (stoichiometric operation) and see how the model can predict the combustion of gasoline-methanol blends starting with the calibration on pure gasoline. The calibration constants are left constant for all the operation points.

The heat transfer multipliers were calibrated for all simulations during the Three Pressure Analysis, based on correspondence between the measured and predicted cylinder pressure, the exhaust and inlet temperatures and the volumetric efficiency. The combustion model was calibrated by minimizing the sum of squared differences between the measured and predicted normalized burn rate. The measured burn rate was derived from the measured cylinder pressure during the Three Pressure Analysis by doing a reverse heat release analysis using the same cylinder model as used in the forward power cycle simulation [16]. The flame development constant C_1 is usually calibrated first in order to get a reasonable correspondence for the ignition delay. As mentioned in [13], increasing C_2 increases the mass entrainment rate, while increasing coefficient C_3 decreases the mass burning rate. Finally, the three constants of the predictive combustion models were simultaneously optimized using the Direct Optimizer embedded in GT-Power [16].

RESULTS

Comparison of laminar burning velocity correlations of pure gasoline – First, a comparison of 4 different laminar burning velocity correlations of gasoline was made: the newly developed correlation based on the measurements of the gasoline used in this study on a flat flame burner, the standard laminar burning velocity correlation for gasoline in the simulation program GT-power [16], the correlation of Gülder [33] and the correlation of Metghalchi & Keck [29]. Figures 1-3 highlight the main differences between the different gasoline or iso-octane (which is often used as gasoline surrogate) laminar burning velocity correlations in terms of equivalence ratio.

As can be seen in Figure 1 the correlation of Gülder considerably overestimates u_l due to uncertainties in the experimental method employed by the author.

In Figure 2, the power exponents α of the temperature dependency are compared. As explained in [27], the power exponent α has a minimum around the equivalence ratio of peak burning velocity which is covered by the newly developed correlation but not by one of the other correlations. The correlation of Metghalchi and Keck predicts a linear decrease of α as function of the equivalence ratio whereas the correlation of Gülder does not include the effect of the equivalence ratio on the power exponent.

The correlation of Gülder does not include the effect of the equivalence ratio on the power exponent β of the pressure dependency either as shown in Figure 3. The other correlations include an increase of β as function of the equivalence ratio.

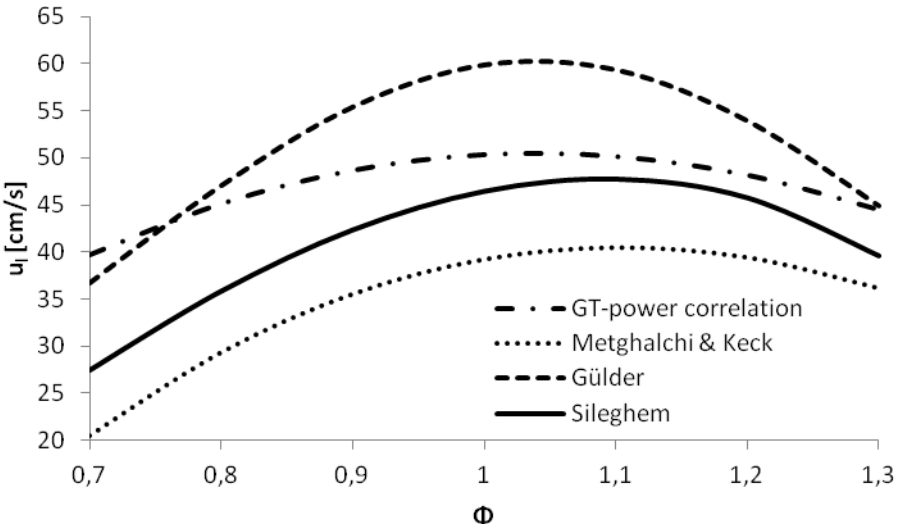

Figure 1 - u_l as a function of ϕ as predicted by several correlations (1bar, 358K).

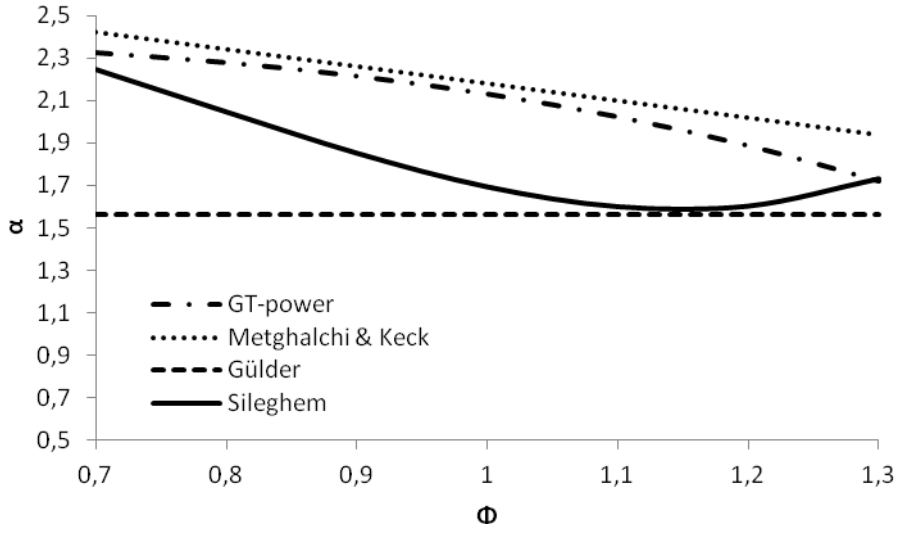

Figure 2 – power exponent α as a function of ϕ as predicted by several correlations

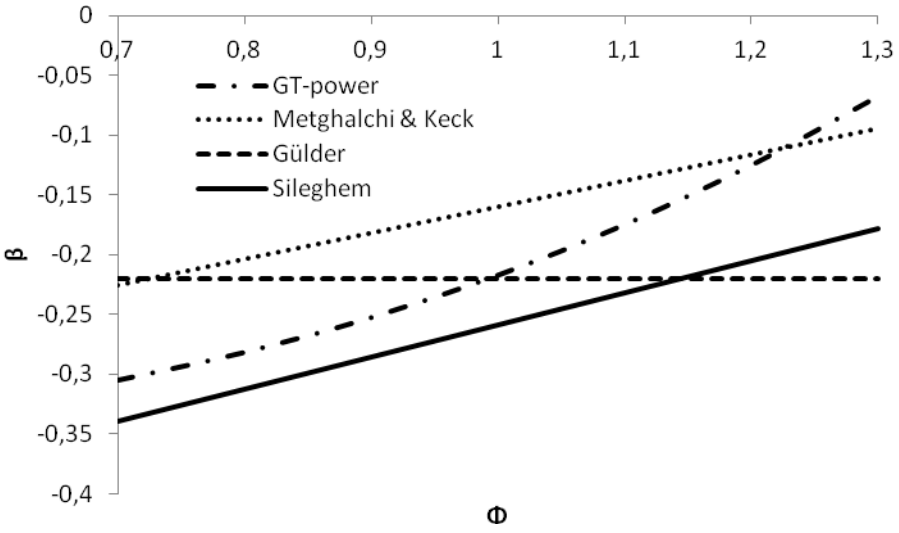

Figure 3 – power exponent β as a function of ϕ as predicted by several correlations

For each correlation, the calibration factors of the simulation program were optimized by minimizing the burn rate RMS error between the measurement at stoichiometry and the simulation. In the bar graphs in Figure 4-7, the error between the simulations at stoichiometry, lean and rich operation are shown for 6 parameters: the ignition delay (0-2% mass fraction burned), duration of 10-90% mass fraction burned, 0-50% mass fraction burned, the maximum pressure, 0-crank angle of maximum pressure and the maximum temperature. As can be seen on the bar graphs, none of the four correlations outperformes the others dramatically. Best agreements are for the newly developed correlation and the standard correlation used in GT-power. As can be seen on the graphs, the error on the ignition delay and 10-90% mass fraction burned has a significant influence on the maximum pressure and the 0-crank angle of maximum pressure. E.g. the more these two burn rate parameters are underpredicted, the more the maximum pressure is overpredicted. We can conclude that in this framework the newly developed correlation performs equally or better than the older correlations. In the next sections this correlation will be used together with the newly developed correlation for methanol.

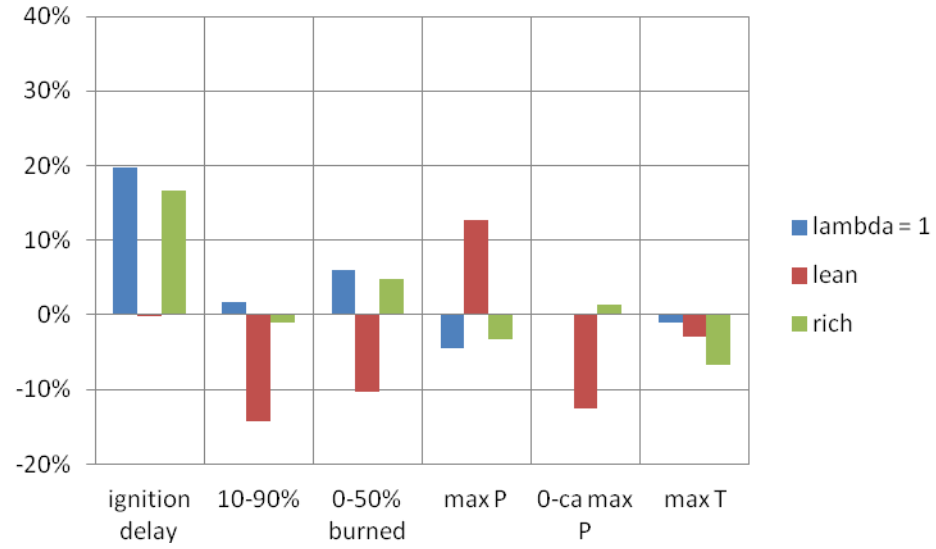

Figure 4 – Simulation error with the gasoline laminar burning velocity correlation of Sileghem.

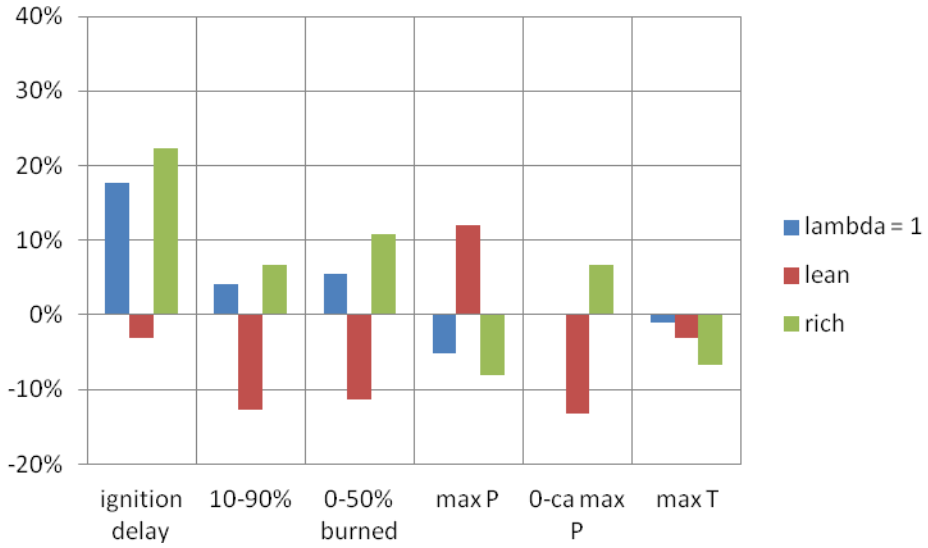

Figure 5 - Simulation error with the gasoline laminar burning velocity correlation of Gt-power.

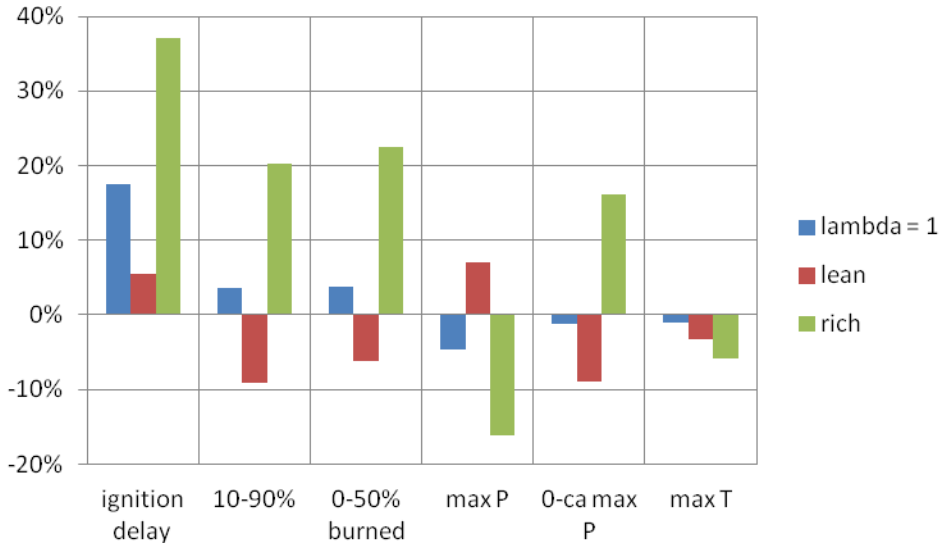

Figure 6 - Simulation error with the gasoline laminar burning velocity correlation of Gülder.

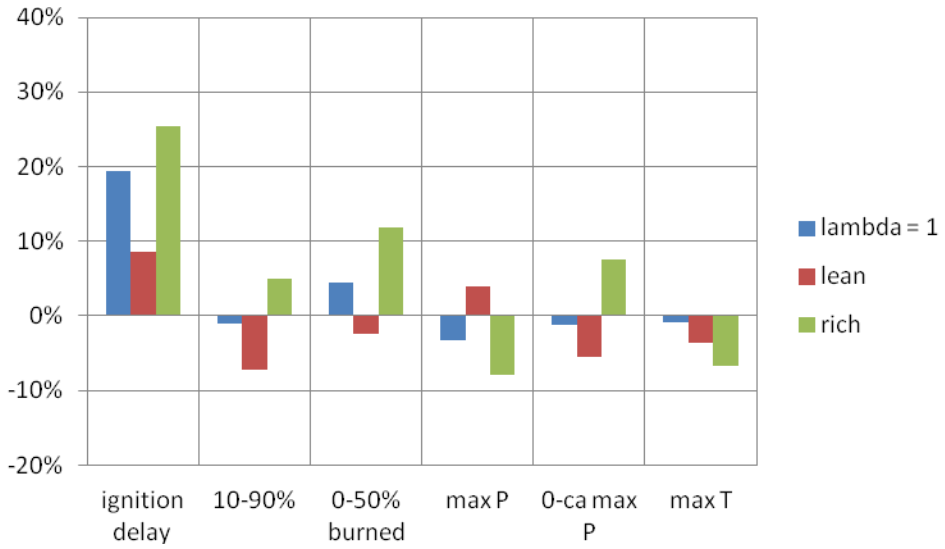

Figure 7 - Simulation error with the gasoline laminar burning velocity correlation of Metghalchi and Keck.

Sensitivity of the simulation program on gasoline - In this section, some parameters of the simulation program will be changed to investigate the sensitivity of the simulation framework on these parameters. The following parameters will be changed: the initial spark size (two times initial kernel radius), the internal EGR fraction, the rms turbulent velocity u' and the integral turbulent length scale Λ. The different parameters have been varied in a range that represents a reasonable estimation of the uncertainty on its value (see Table 2). The sensitivity of the six parameters used in the previous sections is expressed as follows:

$$Sensitivity = \frac{\frac{y(x_0) - y(x_0 + \Delta x)}{y(x_0)}}{\frac{x_0 - (x_0 + \Delta x)}{x_0}} \quad (14)$$

Parameter	**Base value**	Δ
initial kernel radius	0,5 mm	+ 0,5 mm
EGR%	7-9%	+ 3%

u'	~ 2 m/s	+ 1 m/s
Λ	~ 0,0038 m	+ 0,001 m

Table 2 – Parameter values for power cycle sensitivity analysis

A negative value means an opposite change of output with respect to the varied input parameter. Large numbers mean a strong influence of this parameter.
As can be seen on the bar graphs in Figures 8-11, the kernel size has a big influence on the ignition delay and less on the other parameters. This is normal because the spark size determines the initial flame kernel. Later in this study the size of the initial flame kernel (or spark size) will be used to control the ignition delay to be the same as the measured ignition delay in order to study the rest of the combustion process without the influence of the initial flame development.
The second parameter that has been varied is the internal EGR. It has been increased with 3%. This has a significant effect on all the parameters presented here. As a result, the EGR fraction has to be estimated as precisely as possible. That is why a three pressure analysis in GT-power has been used in this study to calculate the internal EGR in the cylinder for each measurement as accurate as possible.
Turbulence quantities are calculated using a very simple turbulence model based on measurements done in a similar engine [18]. The integral length scale Λ is kept constant at 1/5 of the minimum clearance height, and the rms turbulent velocity u' linearly decreases. Confirmation of this turbulence model was not possible during this study. There could be a significant difference between the simple model and the reality. A change in these parameters has a significant effect as can be seen in Figure 10 and Figure 11. Notwithstanding this uncertainty, this turbulence model can be used for the rest of this sensitivity study because throttle position, rpm and ignition timing remain the same for all measurements. The effect of turbulence can be expected to be more or less the same for all the measurements. If for example the engine speed was changed for certain measuring points, more attention should have gone to investigate the change in turbulence as a function of the operating point.

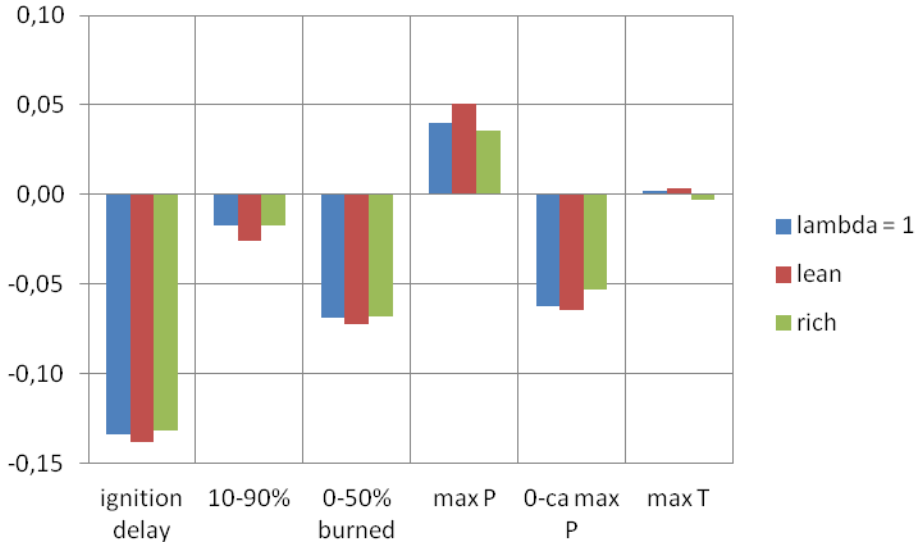

Figure 8 – Sensitivity for a change of the initial kernel radius.

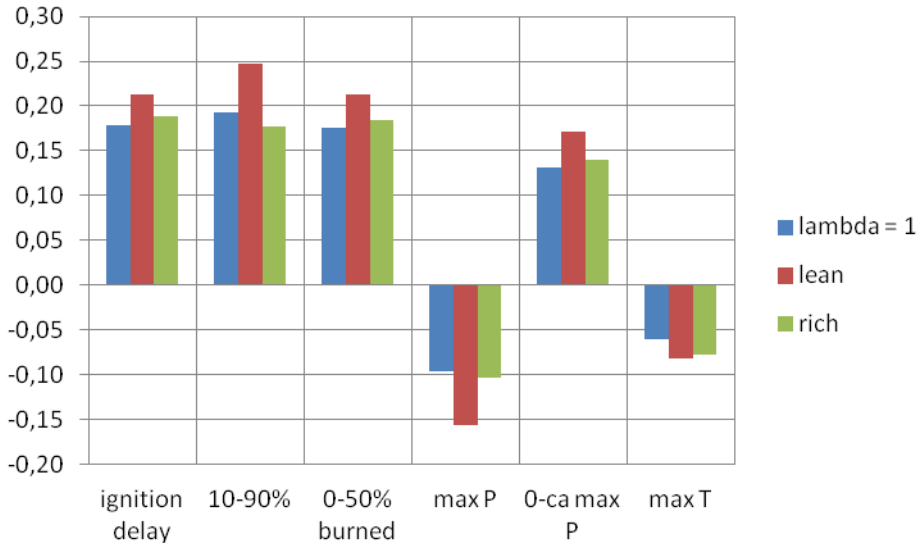

Figure 9 - Sensitivity for a change of the internal EGR percentage

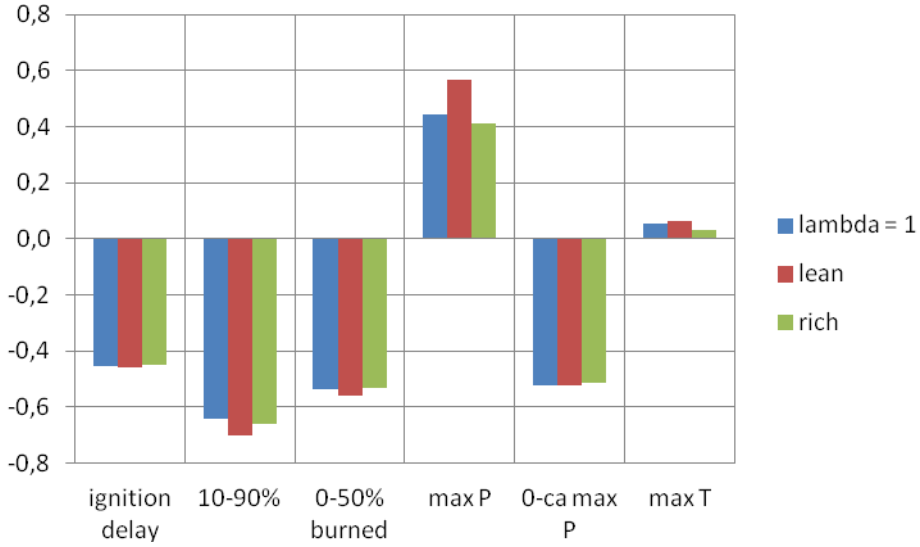

Figure 10 - Sensitivity for a change of the rms turbulent velocity

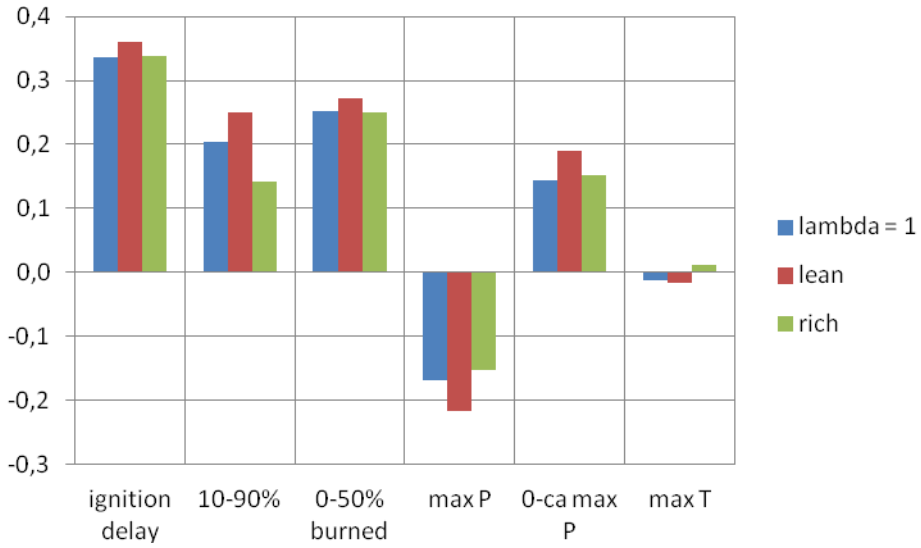

Figure 11 - Sensitivity for a change of the integral length scale

Sensitivity of the simulation program on gasoline-methanol blends – In this section, the predictive capabilities of the simulation program will be evaluated for methanol-gasoline blends using the mixing rule based on energy fraction [26]. The simulation program is again calibrated for stoichiometric operation on gasoline. This is done to investigate how accurate simulations of an engine running on gasoline can be transformed to an engine running on methanol (-alcohol) blends. The influence of the initial flame kernel (spark size) and the internal EGR are again shown. In addition, the effect of changing the temperature power exponent α, the pressure power exponent β and the value of the EGR factor $(1 - \gamma f)$ in the laminar burning velocity correlation of methanol are investigated. The values for gasoline operation remain the same and the influence of changing the parameters of the laminar burning velocity correlation of methanol should become clearer going from gasoline to pure methanol.

Parameter	**Base value**	Δ
initial kernel radius	0,5 mm	+ 0,5 mm
EGR%	7-9%	+ 3%
α	see correlation MeOH	+ 0,07
β	see correlation MeOH	+ 0,05
(1-γf)	see correlation MeOH	- 0,03

Table 3

In Figure 12, the measured ignition delay coming from the burn rate analysis of the three pressure analysis in GT-power is shown together with the predicted ignition delay of the simulation program. On the same Figure, the results of the simulations are shown in which the parameters are changed as in Table 3. The parameters have been varied in a range that represents a reasonable worst case estimation of the uncertainty on its value based on other existing correlations for the laminar burning velocity.
For each operation point, three measurements were done. First the engine was set to a fixed value and the first measurement was done when all the measured values such as exhaust temperature, oil temperature, air flow, etc. did not change anymore. Then, with an interval of a few minutes, a second and third measurement was done. The values shown on the Figures are the mean values of the three measurements and the error bars for the experimental values are calculated by taking two times the standard deviation of the parameter.

As can be seen on Figure 12, the ignition delay at stoichiometric operation is overestimated by the predictive model when the model is calibrated by minimizing the burn rate RMS error of gasoline at stoichiometric operation. Secondly, the experimental ignition delay calculated with a three pressure analysis decreases more than the predicted ignition delay going from gasoline to methanol. As seen on the Figure, changing the initial flame kernel and internal EGR fraction have a significant influence on the ignition delay. When changing the temperature, pressure or EGR dependency of the methanol laminar burning velocity correlation, the biggest change is seen for pure methanol, which is expected. If all the parameters regarding the laminar burning velocity were changed at once, this could have a significant effect. E.g. with the change of the pressure dependency as was done in this study, the correct trend in the ignition delay could be reproduced.

As a result, one of the reasons why the experimental ignition delay decreases with methanol addition cannot be predicted by the predictive model could be that the temperature, pressure or EGR dependency of the laminar burning velocity correlations are not well captured for higher pressure and temperatures in internal combustion engines. Further research should help to decrease the uncertainty of these inputs. Another reason could be that the flame kernel growth model should be adapted for alcohol fuels. At last, there is still uncertainty about the initial flame kernel. The initial flame kernel is defined by the spark size which has a 0.5 mm radius in this simulation framework. As methanol has a lower minimal ignition energy, one could assume that for the same ignition energy input, the initial flame kernel for methanol could be larger.

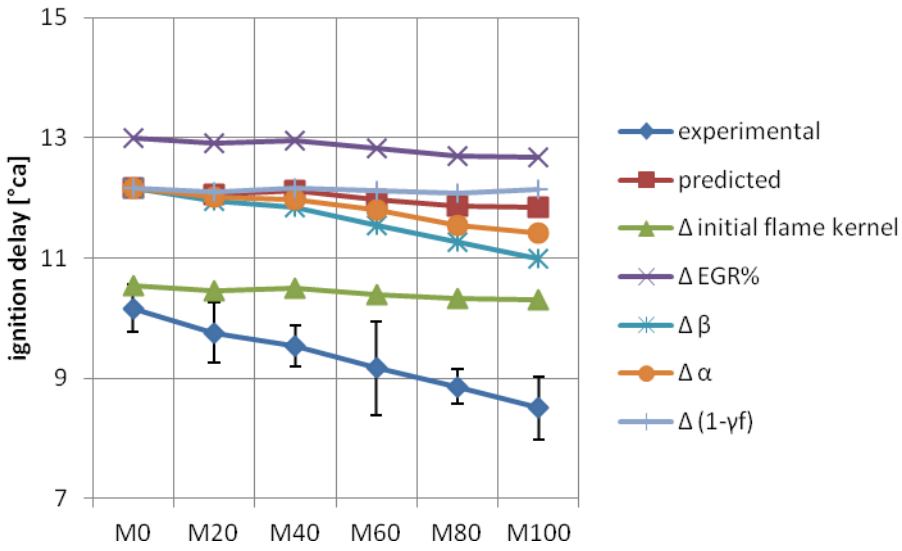

Figure 12 – ignition delay of the stoichiometric mixtures

In Figure 13, the 10-90% mass fraction burned is shown for stoichiometric operation. As can be seen on the Figure, the predictive model overpredicts the burn rate by ~1.5° ca for methanol while the prediction for gasoline is very good. The trend is again not captured enough. There is again a significant change when the internal EGR fraction is changed. The effect of changing the initial flame kernel is much smaller compared to the effect it had on the ignition delay. Due to the change in initial flame kernel, the ignition delay changes as in Figure 12 and this causes the small change in the 10-90% mass fraction burned because of slightly other temperatures and pressure at that moment.

As the flame is more and more developed and because the turbulence flow model does not change going from gasoline to methanol, the difference in burn rate between the fuels is mostly due to the difference in laminar burning velocity. The effect of changing the parameters of the methanol laminar burning velocity correlation can be seen on Figure 13. The correct trend could again be reproduced by changing the parameters of the methanol correlation e.g. the pressure dependency in this case. Additionally, one should note that there exist turbulent burning velocity models that take more fuel properties into account than the turbulent burning velocity model used in this study. This could also have an important influence when simulating the burn rate of fuel blends.

In Figure 14, the 0-50% mass fraction burned is shown. The influence of the ignition delay on the 0-50% mass fraction burned can be seen in this Figure and the same conclusions can be drawn as for the ignition delay. The trend is again best captured in the case where the pressure dependency of the methanol laminar burning velocity correlation is tested. This can also be seen in the maximum pressure data, shown in Figure 15.

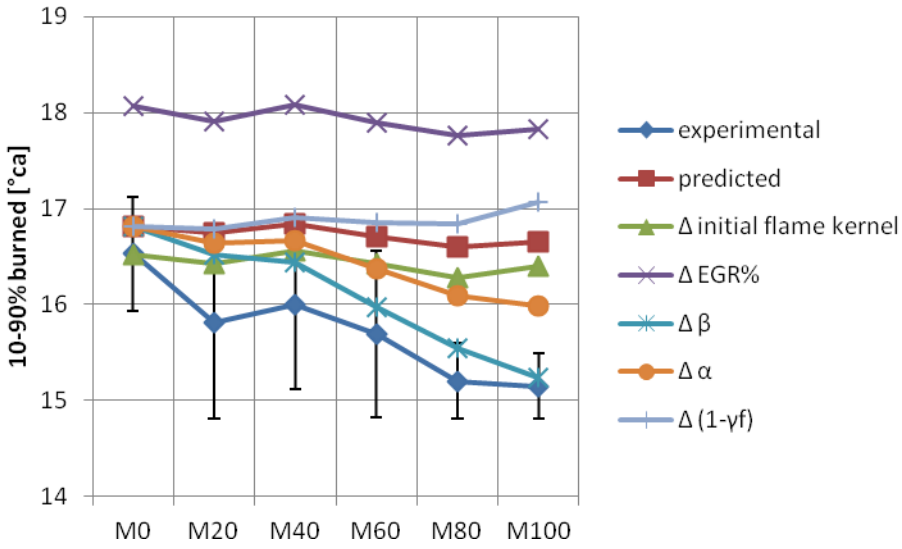

Figure 13 - 10-90% mass fraction burned of the stoichiometric mixtures.

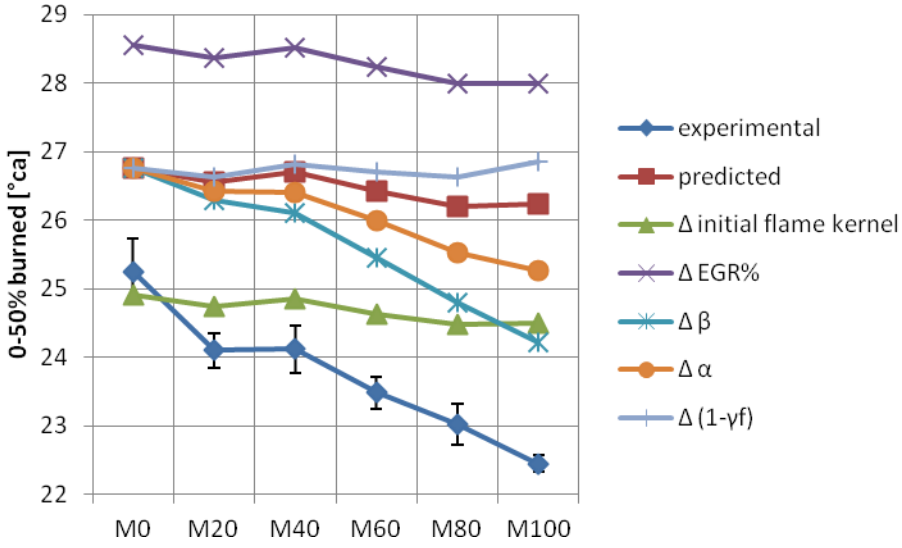

Figure 14 - 0-50% mass fraction burned of the stoichiometric mixtures.

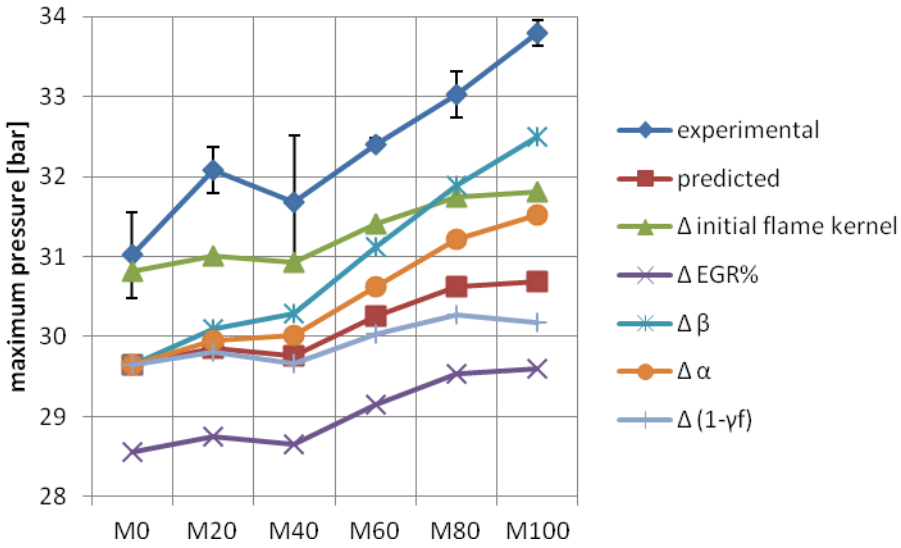

Figure 15 – maximum pressure of the stoichiometric mixtures

For the lean mixtures (see Figures 16-18), more or less the same conclusions can be drawn as for the stoichiometric mixtures. The model does not predict a decrease in ignition delay going from pure gasoline to pure methanol. As a result, the ignition delay is overpredicted for methanol blends with a high methanol content. For rich mixtures (see Figure 19), the ignition delay is overpredicted for all the fuels used in this study but the decreasing trend is better captured. This could be explained by the fact that the developed laminar burning velocity correlations rely on measured data of methanol and gasoline at atmospheric pressure. For rich mixtures, the difference in the measured laminar burning velocity on the flat flame adiabatic burner between methanol and gasoline is significantly larger than for lean or stoichiometric mixtures [26]. Further research should investigate the laminar burning velocity at higher pressures and temperatures. The better prediction of the ignition delay for rich mixtures results in a better prediction for the maximum pressure, see Figure 20.

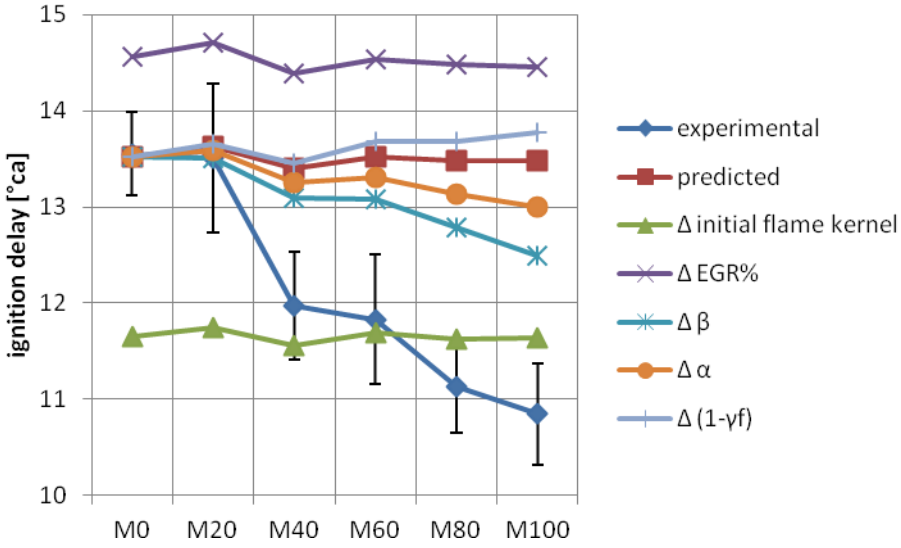

Figure 16 - ignition delay of the lean mixtures

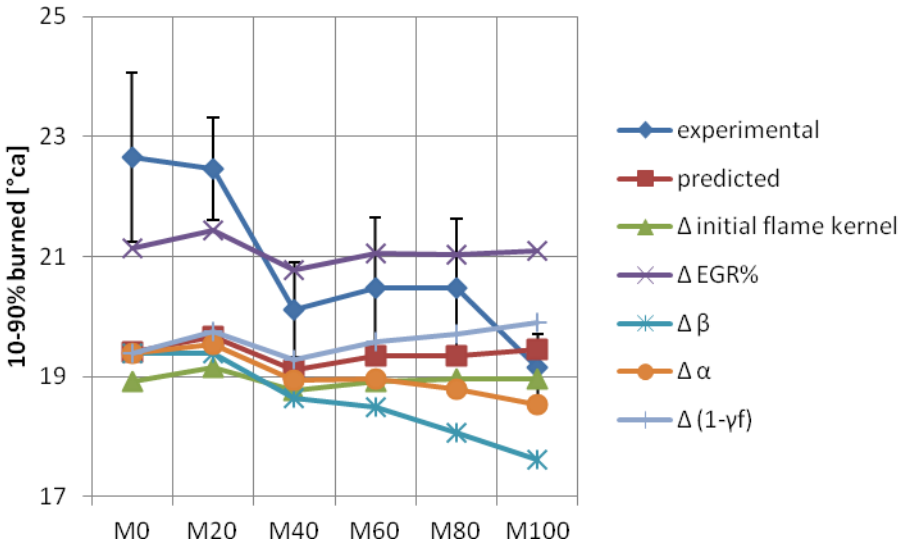

Figure 17 - 10-90% mass fraction burned of the lean mixtures.

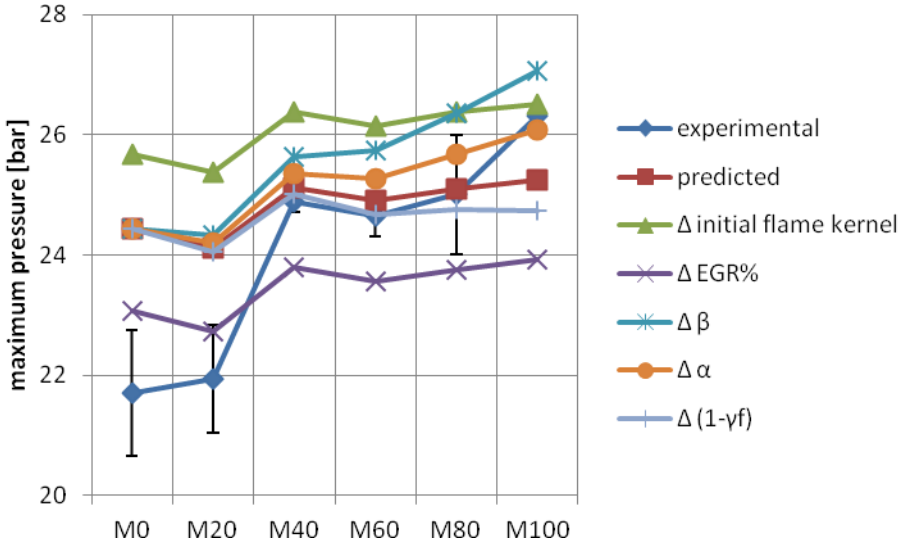

Figure 18 — maximum pressure of the lean mixtures

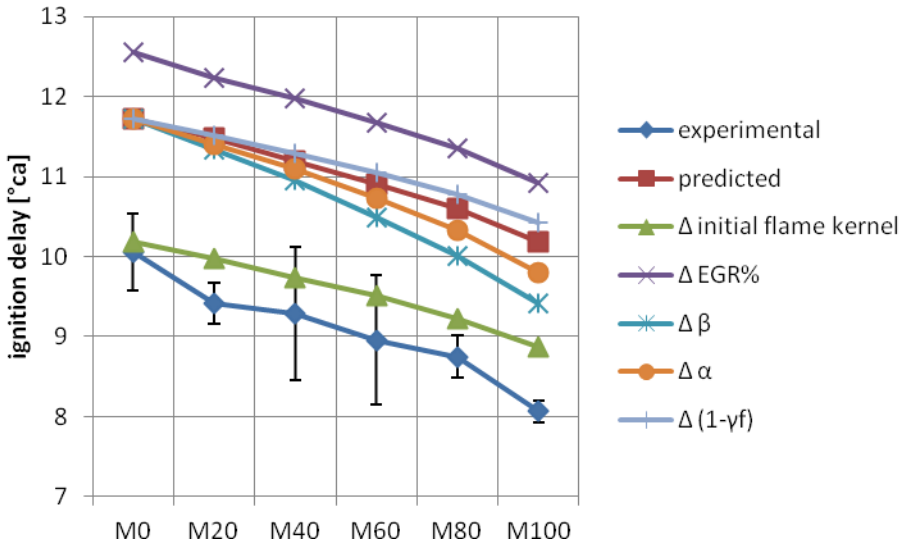

Figure 19 - ignition delay of the rich mixtures

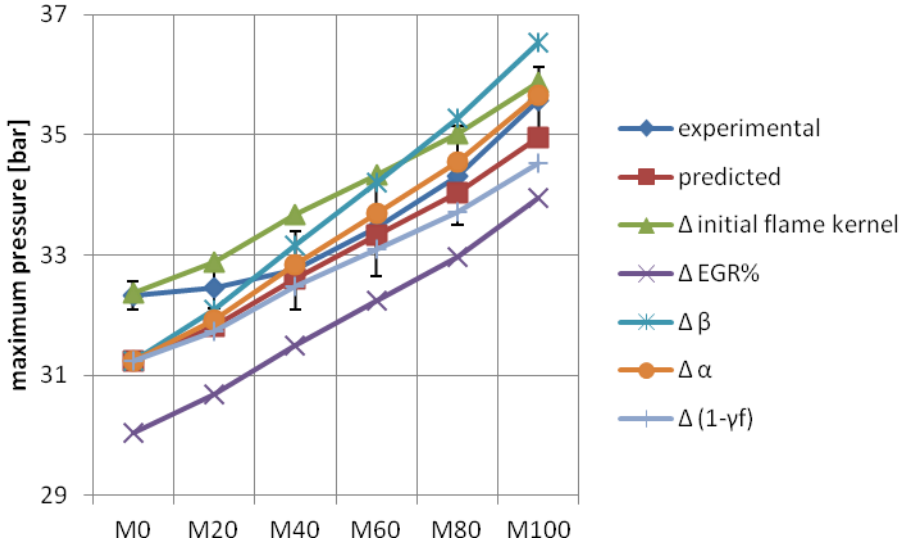

Figure 20 – maximum pressure of the rich mixtures

Optimization of ignition delay of gasoline-methanol blends - One of the main conclusions of the previous section is that the trend of the ignition delay is not well predicted by the simulation model. In this section, an investigation of the simulation model is performed together with an optimization of the ignition delay by changing the initial flame kernel (= spark size). In the first case, the model has been calibrated by changing the calibration factors together with the spark size to minimize the burn rate RMS error of the measurements on gasoline at stoichiometric operation. Then the calibration factors were kept constant while changing the spark size for each individual measurement to minimize the burn rate RMS error. In Figure 21, the results of this optimization are shown for the spark size values. For the stoichiometric and lean mixtures, it is clear that the spark size or initial flame kernel had to be bigger because the ignition delay was not well predicted by the model influencing the rest of the burn rate. For the rich mixtures, the trend of the ignition delay was already well captured and as a result, the spark size stays more or less constant for the fuel range.

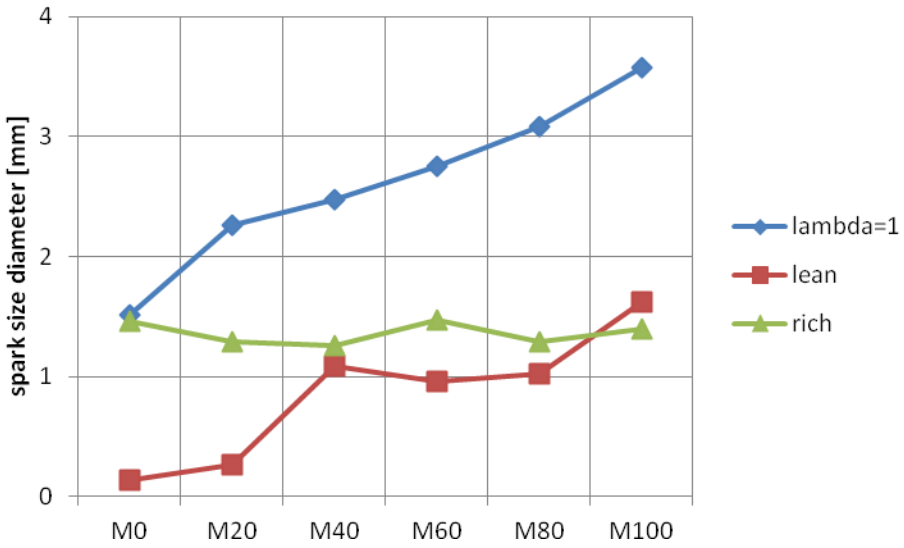

Figure 21 – Spark size diameter for burn rate RMS error optimization.

For the second case, the calibration factors and the spark size are first optimized by minimizing the burn rate RMS error of the measurements on gasoline at stoichiometric operation and then for each measurement the spark size is changed to have the same ignition delay as in the measurements.
In Figure 22, the spark size optimization is shown to simulate the experimental ignition delay. As expected from the previous sections, there is a steeper increase for stoichiometric and lean mixtures going from gasoline to methanol. The spark timing for rich mixtures stays again relatively constant. It is notable that the spark timing for lean mixtures follows the same trend as the stoichimetric mixtures but that all values are lower. This could be explained by the fact that lean mixtures are harder to ignite than stoichiometric mixtures. This result requests for a more fuel independent flame development model or a more fuel independent initial flame model.

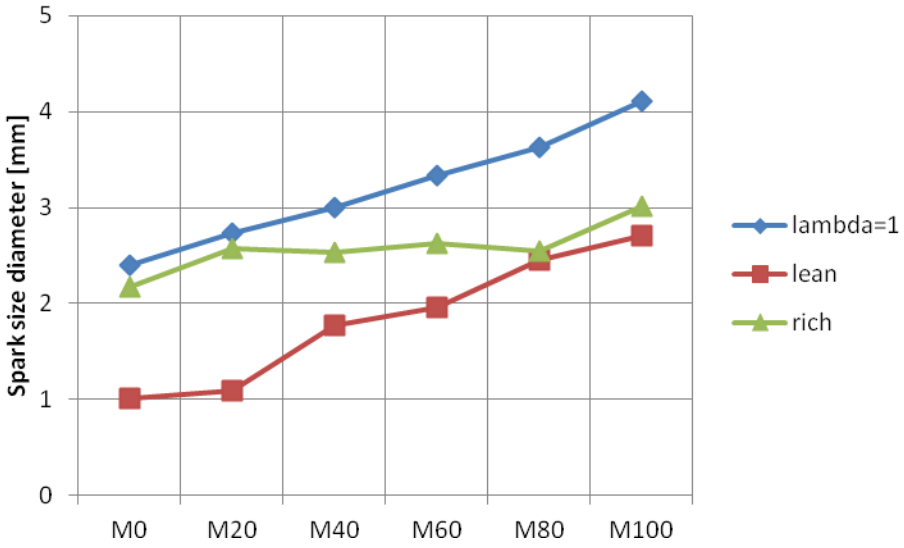

Figure 22 - Spark size diameter for ignition delay optimization.

When the ignition delay is not an issue anymore, it is easier to evaluate the predictive capabilities regarding the other parameters. In Figure 23, Figure 24 and Figure 25, the 10-90% mass fraction burned, the maximum pressure and the 0-50% mass fraction burned for the stoichiometric mixtures are shown for the simulations with optimized ignition delay. For the 10-90% mass fraction burned, the trend is very similar to the simulations without the ignition delay optimization. There is a small change in the 10-90% mass fraction burned because of slightly other temperatures and pressure. The agreement with the experimental maximum pressure and the 0-50% mass fraction burned is much better due to the optimized ignition delay. This results in smaller burn rate RMS error for the methanol-gasoline blends. This can be seen in Figure 26. It is clear that the agreement is much better for the fuel with high methanol content. Only for pure gasoline the error is larger because originally the model was calibrated to have a minimum error.

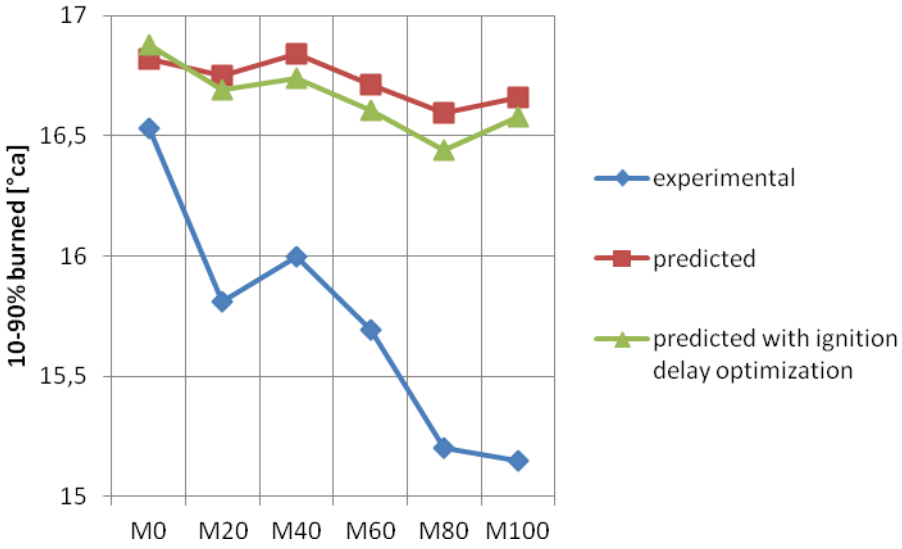

Figure 23 – 10-90% mass fraction burned of the stoichiometric mixtures with ignition delay optimization

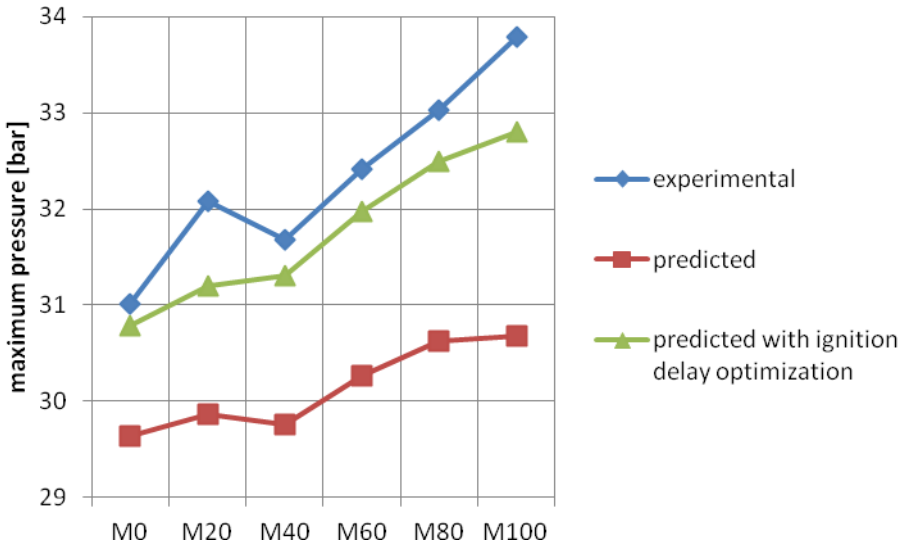

Figure 24 – maximum pressure of the stoichiometric mixtures with ignition delay optimization

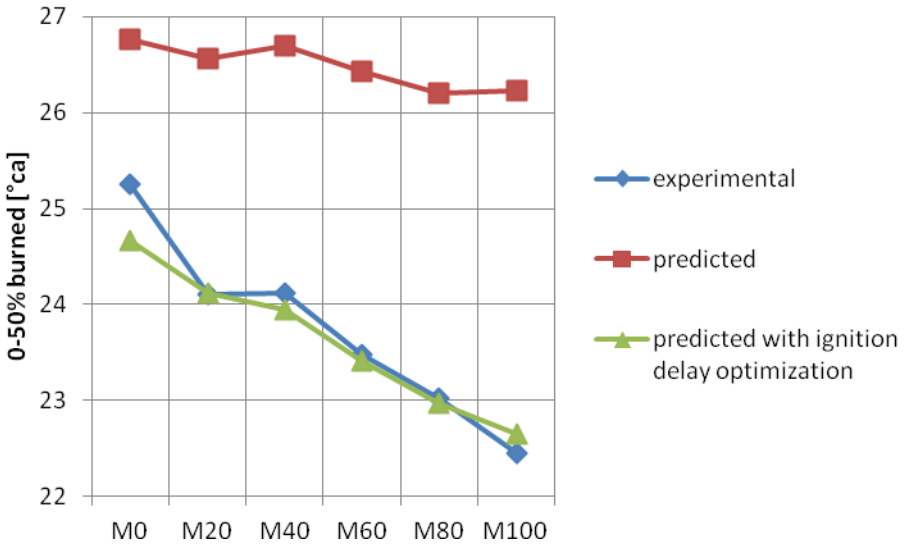

Figure 25 – 0-50% mass fraction burned of the stoichiometric mixtures with ignition delay optimization

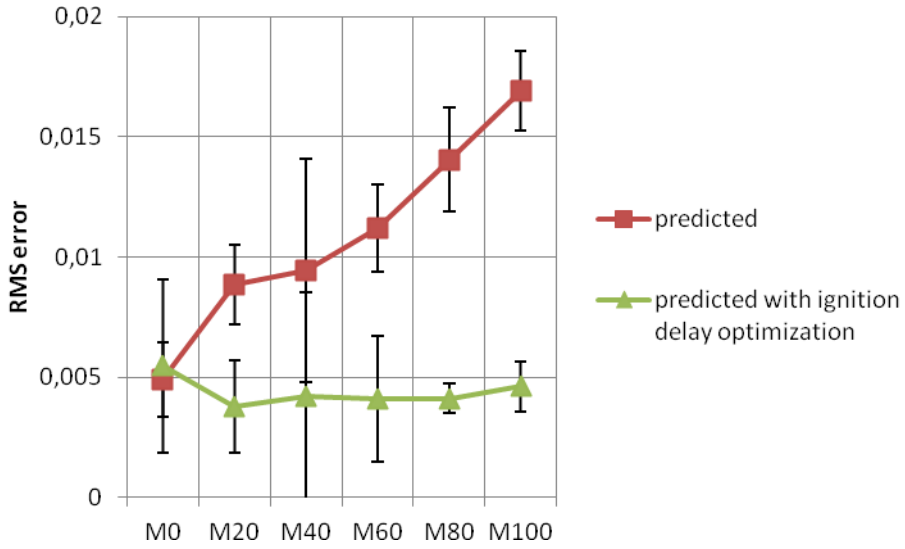

Figure 26 – burn rate RMS error of the stoichiometric mixtures with ignition delay optimization

Finally, simulations have been done with a methanol laminar burning velocity correlation from another source. The laminar burning velocity correlation of Gülder was used here:

$$u_l = u_{l0}\left(\frac{T_u}{T_0}\right)^{\alpha}\left(\frac{p}{p_0}\right)^{\beta}(1-\gamma f)$$

with

$$u_{l0} = 0.492\phi 0.25 exp\left(-5.11(\phi-1.075)^2\right)$$

$$\alpha = 1.75$$

$$\beta = -0.2\phi \; if \; \phi > 1$$

$$\beta = -\frac{0.2}{\sqrt{\phi}} \; if \; \phi \leq 1$$

In this equation T_0 is 300K and p_0 is 1bar. The same value of 2.1 has been taken for the EGR factor γ as in the newly developed equations.

As can be seen in the Figure 27, 28 and 29, this laminar burning velocity has a big influence on the results of pure methanol. Especially at stoichiometric operation, the laminar burning velocity prediction of this correlation is different resulting in an overestimation of the burn rate and peak pressure.

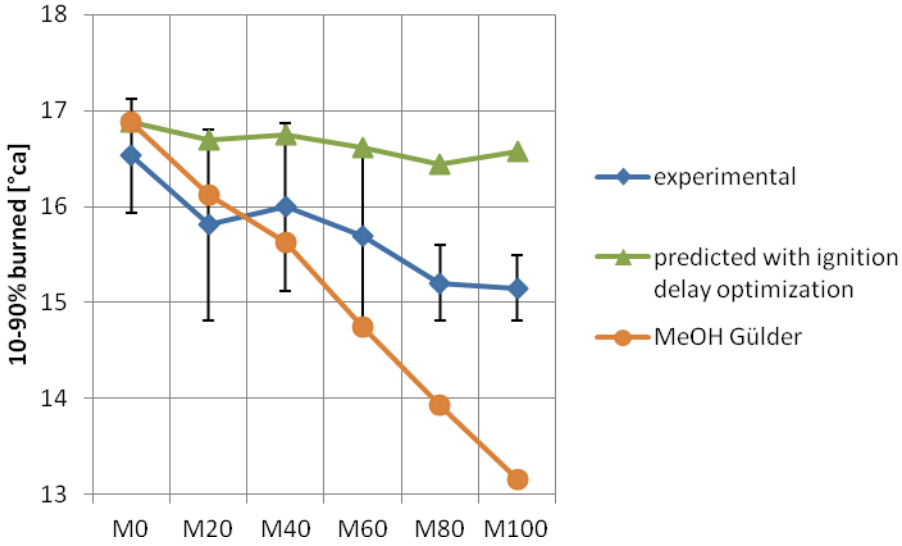

Figure 27 – 10-90% mass fraction burned of the stoichiometric mixtures with methanol laminar burning velocity correlation of Gülder

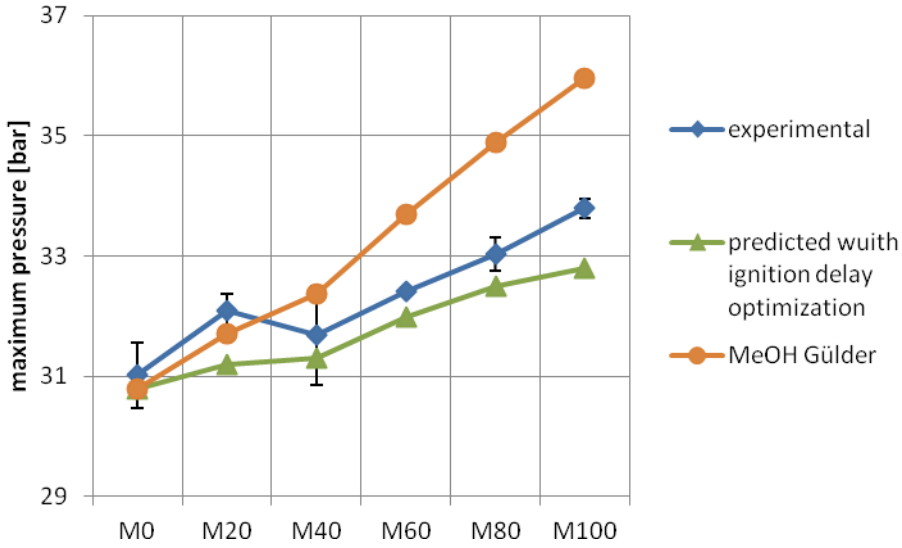

Figure 28 – maximum pressure of the stoichiometric mixtures with methanol laminar burning velocity correlation of Gülder

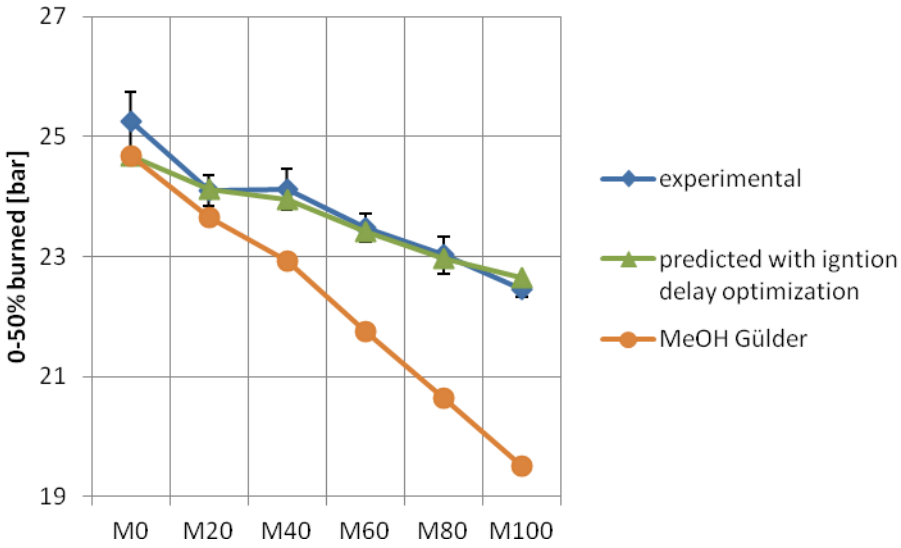

Figure 29 – 0-50% mass fraction burned of the stoichiometric mixtures with methanol laminar burning velocity correlation of Gülder

CONCLUSIONS

The focus of the current paper was the development and validation of a quasi-dimensional model for the combustion of methanol-gasoline blends in spark-ignition engines. The predictive performance of newly developed laminar burning velocity correlations for gasoline and methanol together with a mixing rule was assessed.

First, a comparison of 4 different laminar burning velocity correlations of gasoline was made and the newly developed correlation performed equally or better than the older correlations. Secondly, the sensitivity of certain parameters was shown. It resulted that the EGR fraction has to be estimated as precisely as possible. That is why a three pressure analysis in GT-power has been used in this study to calculate the internal EGR fraction in the cylinder for each measurement. Thirdly, the sensitivity was investigated for fuel blends going from pure gasoline to pure methanol. The results show the importance of the laminar burning velocity correlation, the initial flame kernel and the estimation of the residual gas fraction. The trend of the experimental ignition delay was not reproduced in the simulations. After optimizing the spark size to have the same ignition delay as in the measurements, the trends in burn rate and peak pressures were much better reproduced. As a result, we can conclude that there is a need for a fuel independent flame kernel growth model probably together with a submodel that can predict the trends in the initial flame kernel size as a function of the spark plug energy, the air to fuel ratio at the spark plug and the fuel. Current predictive combustion simulations could benefit from an initial flame kernel size multiplier (or a spark size multiplier) as a function of the spark plug energy, the air to fuel ratio and the fuel.

ACKNOWLEDGEMENTS - L. Sileghem and J. Vancoillie gratefully acknowledge a Ph. D. fellowship of the Research Foundation - Flanders (FWO11/ASP/056 and FWO09/ASP/030). The authors would like to thank BioMCN for providing the bio-methanol used in this study.

REFERENCES

[1] J. Vancoillie, J. Demuynck, L. Sileghem, M. Van De Ginste, S. Verhelst, L. Brabant, L. Van Hoorebeke, The potential of methanol as a fuel for flex-fuel and dedicated spark-ignition engines, Applied Energy, 102 (2013) 140-149.

[2] On the promotion of the use of energy from renewable sources and amending and subsequently repealing Directives 2001/77/EC and 2003/30/EC. Directive 2009/28/EC of the European Parliament and of the Council; 23rd April 2009.
[3] Energy Independence and Security Act of 2007. Public Law 110-140. In: 110th Congress, DOCID: f:publ140.110; 2007.
[4] R.J. Pearson, J.W.G. Turner, A.J. Peck, Gasoline-ethanol-methanol tri-fuel vehicle development and its role in expediting sustainable organic fuels for transport, in: IMechE Low Carbon Vehicles Conference, London, UK, 2009, pp. 1-21.
[5] Turner, J., Pearson, R., Purvis, R., Dekker, E. et al., "GEM Ternary Blends: Removing the Biomass Limit by using Iso-Stoichiometric Mixtures of Gasoline, Ethanol and Methanol," SAE Technical Paper 2011-24-0113, 2011, doi:10.4271/2011-24-0113.
[6] Specht M, Bandi A. Renewable carbon-based transportation fuels. Berlin Heidelberg, Berlin: Springer; 2006.
[7] Pearson RJ, Eisaman MD, Turner JWG, Edwards PP, Jiang Z, Kuznetsov VL, Littau KA, et al. Energy storage via carbon-neutral fuels made from CO2, water, and renewable energy. In: Proceedings of the IEEE, vol. 100; 2012. p. 440–60.
[8] Olah GA, Goeppert A, Prakash GK. Beyond oil and gas: the methanol economy. Weinheim, Germany: Wiley-VCH Verlag CmbH & Co., KGaA; 2006.
[9] Ward PF, Teague JM. Fifteen years of fuel methanol distribution. In: 11th International symposium on alcohol fuels Sun City, South, Africa; 1996.
[10] J. Vancoillie, J. Demuynck, L. Sileghem, M.V.D. Ginste, S. Verhelst, L. Brabant, L.V. Hoorebeke, The potential of methanol as a fuel for flex-fuel and dedicated spark-ignition engines, Applied Energy, (2012).
[11] L. Sileghem, A. Coppens, B. Casier, J. Vancoillie, S. Verhelst, Performance and emissions of iso-stoichiometric ternary GEM blends on a production SI engine, Fuel, 117, Part A (2014) 286-293.
[12] S. Verhelst, C.G.W. Sheppard, Multi-zone thermodynamic modelling of spark-ignition engine combustion - An overview, Energy Conversion and Management, 50 (2009) 1326-1335.
[13] S. Verhelst, R. Sierens, A quasi-dimensional model for the power cycle of a hydrogen-fuelled ICE, International Journal of Hydrogen Energy, 32 (2007) 3545-3554.
[14] S. Verhelst, A study of the combustion in hydrogen-fuelled internal combustion engines. PhD thesis, Department of Flow, Heat and Combustion mechanics, Ghent University, Ghent, Belgium, 2005.
[15] J. Vancoillie, Modeling the combustion of light alcohols in spark-ignition engines. PhD thesis, Department of Flow, Heat and Combustion mechanics, Ghent University, Ghent, Belgium, 2013.
[16] GammaTechnologies, "GT-Suite Version 7.3 User's Manual ", 2013.
[17] Morel, T., Rackmil, C., Keribar, R., and Jennings, M., "Model for Heat Transfer and Combustion In Spark Ignited Engines and its Comparison with Experiments," SAE Technical Paper 880198, 1988, doi:10.4271/880198.
[18] Hall, M. and Bracco, F., "A Study of Velocities and Turbulence Intensities Measured in Firing and Motored Engines," SAE Technical Paper 870453, 1987, doi:10.4271/870453.
[19] Wahiduzzaman, S., Moral, T., and Sheard, S., "Comparison of Measured and Predicted Combustion Characteristics of a Four-Valve S.I. Engine," SAE Technical Paper 930613, 1993, doi:10.4271/930613.
[20] Bougrine, S., Richard, S., and Veynante, D., "Modelling and Simulation of the Combustion of Ethanol blended Fuels in a SI Engine using a 0D Coherent Flame Model," SAE Technical Paper 2009-24-0016, 2009, doi:10.4271/2009-24-0016.
[21] Ö.L. Gülder, Burning Velocities Of Ethanol Isooctane Blends, Combustion and Flame, 56 (1984) 261-268.
[22] F. Ma, Y. Wang, M. Wang, H. Liu, J. Wang, S. Ding, S. Zhao, Development and validation of a quasi-dimensional combustion model for SI engines fuelled by HCNG with variable hydrogen fractions, International Journal of Hydrogen Energy, 33 (2008) 4863-4875.
[23] F. Perini, F. Paltrinieri, E. Mattarelli, A quasi-dimensional combustion model for performance and emissions of SI engines running on hydrogen–methane blends, International Journal of Hydrogen Energy, 35 (2010) 4687-4701.
[24] V. Di Sarli, A. Di Benedetto, Laminar burning velocity of hydrogen-methane/air premixed flames, International Journal of Hydrogen Energy, 32 (2007) 637-646.
[25] L. Sileghem, J. Vancoillie, J. Demuynck, J. Galle, S. Verhelst, Alternative Fuels for Spark-Ignition Engines: Mixing Rules for the Laminar Burning Velocity of Gasoline–Alcohol Blends, Energy & Fuels, 26 (2012) 4721-4727.
[26] L. Sileghem, V.A. Alekseev, J. Vancoillie, E.J.K. Nilsson, S. Verhelst, A.A. Konnov, Laminar burning velocities of primary reference fuels and simple alcohols, Fuel, 115 (2014) 32-40.
[27] L. Sileghem, V.A. Alekseev, J. Vancoillie, K.M. Van Geem, E.J.K. Nilsson, S. Verhelst, A.A. Konnov, Laminar burning velocity of gasoline and the gasoline surrogate components iso-octane, n-heptane and toluene, Fuel, 112 (2013) 355-365.
[28] B. Galmiche, F. Halter, F. Foucher, Effects of high pressure, high temperature and dilution on laminar burning velocities and Markstein lengths of iso-octane/air mixtures, Combustion and Flame, 159 (2012) 3286-3299.
[29] M. Metghalchi, J.C. Keck, Burning velocities of mixtures of air with methanol, isooctane, and indolene at high pressure and temperature, Combustion and Flame, 48 (1982) 191-210.
[30] D. Bradley, M. Lawes, K. Liu, S. Verhelst, R. Woolley, Laminar burning velocities of lean hydrogen-air mixtures at pressures up to 1.0 MPa, Combust. Flame, 149 (2007) 162-172.
[31] Z. Zhang, Z. Huang, X. Wang, J. Xiang, X. Wang, H. Miao, Measurements of Laminar burning velocity and Markstein lengths for methanol-air-nitrogen mixtures at elevated pressures and temperatures, Combustion and Flame, 155 (2008) 358-368.

[32] J. Demuynck, M. De Paepe, H. Huisseune, R. Sierens, J. Vancoillie, S. Verhelst, Investigation of the influence of engine settings on the heat flux in a hydrogen- and methane-fueled spark ignition engine, Applied Thermal Engineering, 31 (2011) 1220-1228.
[33] Gülder, Ö., "Correlations of Laminar Combustion Data for Alternative S.I. Engine Fuels," SAE Technical Paper 841000, 1984, doi:10.4271/841000.